

## Research Article

# Evaluating the Performance of Connected and Automated Vehicles in Fixed Signal-Controlled Conventional Intersections and Superstreets with Platooning-Based Trajectory Planning

Shaojie Liu<sup>1</sup> and Wei David Fan <sup>2</sup>

<sup>1</sup>USDOT Center for Advanced Multimodal Mobility Solutions and Education (CammSE),  
Department of Civil and Environmental Engineering, University of North Carolina at Charlotte, 9201 University City,  
Charlotte 28223, NC, USA

<sup>2</sup>USDOT Center for Advanced Multimodal Mobility Solutions and Education (CammSE),  
Department of Civil and Environmental Engineering, University of North Carolina at Charlotte, 9201 University City Blvd,  
Charlotte 28223, NC, USA

Correspondence should be addressed to Wei David Fan; [wfan7@uncc.edu](mailto:wfan7@uncc.edu)

Received 5 March 2022; Revised 6 May 2022; Accepted 14 May 2022; Published 2 June 2022

Academic Editor: Yanyan Qin

Copyright © 2022 Shaojie Liu and Wei David Fan. This is an open access article distributed under the Creative Commons Attribution License, which permits unrestricted use, distribution, and reproduction in any medium, provided the original work is properly cited.

Connected and autonomous vehicles (CAVs) are emerging technology that attracts the interests of many transportation professionals and computational scientists. Several recent studies have investigated different model frameworks of CAVs in different transportation environments, such as on freeways and at conventional intersections. Nevertheless, few efforts have been made to investigate the performances of CAVs at innovative intersections, and the lack of knowledge can result in an inaccurate prediction of CAVs performances in the existing transportation network. This research intends to mitigate this research gap by studying the traffic delay and fuel consumption of CAVs in the environment of the superstreet and its equivalent conventional intersection through simulation-based experiments. A real-world superstreet in Leeland, NC, is selected and used. A conventional intersection with equivalent road designs is established in the simulation platform to make a comparison with the selected superstreet. This research develops both platooning and trajectory planning modeling frameworks to examine the implications of CAVs with different capabilities. The Intelligent Driver Model (IDM) is selected and applied to model the CAV behaviors, while Wiedemann 99 (W99) is used to model Human-Driven Vehicles (HDVs). The simulation results demonstrate the efficiency of both platooning and trajectory planning, respectively. Different effects of CAVs in the superstreet and its equivalent conventional intersection are observed. The findings from this research can provide an important reference for transportation planners and policymakers in predicting the influence of CAVs on the existing transportation infrastructure.

## 1. Introduction

CAVs are promising technology and can yield significant impacts in various transportation environments. Extensive efforts have been devoted to exploring the potential effects of CAVs in various transportation environments, including freeways [1–3], roundabouts [4, 5], and conventional intersections [6, 7]. In these studies, assumptions were often made for CAVs' capabilities, such as trajectory planning, shorter headways, accurate controls, shorter reaction times, and communication with other vehicles or infrastructure,

such as traffic signals [8, 9]. However, few efforts have been devoted to investigating the impact of CAVs on the operational performance of innovative intersections. Among the numerous innovative intersection designs, superstreet is one of them that has been successfully implemented in several places in the US [10].

Therefore, this research intends to mitigate the research gap by exploring the different performances of CAVs in the environments of the superstreet and conventional intersection. The research uses Simulation of Urban Mobility (SUMO) as the simulation platform due to its rich

Application Programming Interfaces (APIs) to build proper behavior models of CAVs and HDVs. To be specific, different car-following models are considered for CAVs and HDVs, respectively. To account for the car-following characteristics of HDVs, W99 is selected for its consideration of both mechanical features of vehicles and the randomness of human drivers. As for CAVs, IDM is selected and used due to its intuitive measurable parameters and accurate controls of vehicle movements. This research also takes account of popular advanced features of CAVs including platooning and trajectory planning strategies. A superstreet from North Carolina in the real world is selected for the case study for its typical superstreet design and traffic flow characteristics. An equivalent conventional intersection with a similar road configuration is also designed and used in the same simulation platform to make a fair comparison. The performance evaluation also explicitly accounts for different traffic demands and market penetration rates.

The rest of the paper is laid out as follows: First, this research gives a brief literature review on the superstreet and CAVs technology, respectively. Second, this paper introduces the modeling framework for CAVs and HDVs, especially for the behavior models of CAVs. Third, this paper presents and discusses relevant results generated from the designed scenarios. Then conclusions are drawn based on the research findings.

## 2. Literature Review

Superstreet is one of the popular innovative intersection designs which has been applied in numerous places, especially in the states of North Carolina and Maryland in the US [10]. By allocating more green time for vehicles from the main road, superstreets could yield less traffic delay compared to conventional intersections, especially when there are significant unbalanced traffic volumes between the main road and the minor road [11, 12]. Hummer et al. [13] conducted a study investigating a superstreet corridor situated in North Carolina. Conclusions were made that the superstreet could potentially yield travel time and safety benefits. In addition to the studies on the performance's comparison between superstreet and its equivalent conventional intersection, Xu et al. [14, 15] investigated the optimal design of U-turn offset length and signal timing plan using an analytical approach and optimization methods, respectively.

In recent years, CAVs have become promising solutions to reduce congestion at intersections due to their shorter headways and trajectory guidance capabilities. The performances of CAVs are robust in different transportation scenarios, and they can consistently yield less travel time, traffic delay, and fuel consumption [7, 16, 17]. Table 1 provides a summary of recent existing studies on CAVs categorized by transportation environments.

CAVs and HDVs are often modeled with different car-following models. On the one hand, W99 is the popular HDV model for its rich parameters that capture the randomness of human driver behaviors [1, 28]. On the other hand, CAVs can be modeled with IDM, the adaptive cruising control (ACC) model, or the cooperative adaptive cruising control

(CACC) model. These models all have intuitive measurable parameters for CAVs. CACC model is developed based on the ACC model by adding two-way communication between the preceding vehicles and the following vehicles. With CACC, the CAVs can travel on the roads with shorter headways (0.6s) compared to ACC vehicles [29].

Platooning is a unique feature for CAVs for its communication capabilities with other vehicles. A platoon of CAVs can travel on the roads with homogenous speeds and shorter headways [30]. Moreover, when it comes to planning trajectories, researchers only need to determine the trajectories of leading vehicles, and the rest of the vehicles inside the platoon can follow the trajectory of the leading vehicle. Different studies may have different definitions for the platoon. Feng et al. [31] and Yu et al. [32] defined the platoon as a group of vehicles that can travel through the intersection within one phase, while Ye et al. [33] defined the platoon as a group of vehicles that share similar speeds and have a close distance in between. In addition, some studies specifically defined the car-following behaviors of the vehicles inside the platoon [34, 35].

With trajectory planning, CAVs can follow a calculated velocity or acceleration/deceleration rate at each time step when approaching the intersection. The calculated velocity/acceleration profiles may achieve certain optimal traffic performance measures such as minimal travel time, fuel consumption, or emissions [31–33]. When the objectives are fuel consumption or carbon dioxide emissions, the objective functions often result in a nonlinear function form whose analytical solutions are hard to obtain. Hence, nonlinear programming, dynamic programming, and other meta-heuristic methods like the genetic algorithm (GA) are popular approaches to solving such problems [32, 33, 36, 37]. Nevertheless, computational efficiency is an inevitable great challenge in the real world when these approaches are in deployment. Notably, trajectory planning that is combined with signal optimization can eliminate vehicle stops [31, 32]. Adaptive signal controls with knowledge of vehicle arrival patterns may perform significantly better than trajectory planning standalone. Nevertheless, the combined optimization of trajectory planning and signal timing has limitations in the requirement of the full market penetration rate of CAVs and considerable investment in the hardware installation and maintenance of traffic lights. Thus, this joint coordination between the traffic light and CAVs is likely to be implemented in the latter stages of CAV development. In an environment where adaptive signals are not available, Green Light Optimal Speed Advisory (GLOSA) was proposed in the fixed signal-controlled intersections [38, 39]. With GLOSA, an optimal speed could be determined for CAVs based on the remaining green time or the green phase initiation time to reduce the number of stops or total waiting time.

Through literature review, a general modeling framework of CAVs and HDVs can be identified. This research adopts concepts including car-following models, platooning, and trajectory planning to model the behaviors of CAVs. Also, it is found that few studies have been conducted on investigating the CAVs' performances in innovative intersections. By simulating the HDVs and CAVs in the environment of the superstreet and equivalent conventional

TABLE 1: Recent studies on the CAVs categorized by transportation environments.

Transportation environments	Authors	Year	CAV features
<i>Freeway</i>	Guo et al. [3]	2020	CACC, platoons, cooperative merging
	Adebisi et al. [18]	2020	CACC models
	Liu and Fan [1]	2020	CAVs with revised intelligent driver model
	Chityala et al. [19]	2020	CAVs with shorter headways
	Hu and Sun [20]	2019	Cooperative lane changing control, cooperative merging control
<i>Conventional intersection</i>	Han et al. [7]	2020	Platooning-based trajectory planning with optimal control framework
	Pourmehrhab et al. [21]	2020	CAVs with an intelligent intersection control algorithm (IICA) and hybrid autonomous intersection management (H-AIM)
	Guo et al. [22]	2019	Joint optimization of vehicle trajectory and intersection controller with combined dynamic programming and shooting heuristic approach
	Li and Zhou [23]	2017	Signal timing optimization with the brand and bound algorithm considering mixed traditional vehicles
	Zhou et al. [24]	2017	Parsimonious shooting heuristics algorithm to construct vehicle trajectories on a signalized highway segment
<i>Roundabout</i>	Jiang et al. [6]	2017	Eco approaching at an isolated signalized intersection under partially connected and automated vehicles environment
	Dresner and Stone [25]	2008	Reservations based algorithm in the lightless intersection
	Mohebifard and Hajbabaie [4]	2021a	Optimization on trajectory and merging sequence; customized solution technique that transforms the two-dimensional optimization problem into a combination of easier one- and two-dimensional subproblems
	Mohebifard and Hajbabaie [5]	2021b	Trajectory control in a roundabout with a mixed fleet of automated and human-driven vehicles
	Martin-Gasulla and Elefteriadou [26]	2021	Roundabout management algorithm for trajectory planning of CAVs
Chalaki et al. [27]	2020	Trajectory planning control framework for roundabout	

intersection, this research can close the identified research gap and provide an important reference for policymakers.

### 3. Methodology

This section illustrates the methodology of modeling HDVs and CAVs procedures. The researchers utilize the W99 model that is calibrated by GA to model the HDVs in superstreets, while CAVs are modeled with IDM. Moreover, platooning and trajectory planning schemes are also developed for CAVs.

#### 3.1. Information on the Selected Location for Case Study.

A superstreet situated in Leland, NC is identified for the case study. This superstreet is selected for its typical geometric design and traffic flow characteristics. The traffic characteristic information on the selected superstreet is available in Hummer et al. [13]. Figure 1 shows the selected superstreet and signal locations in Google Maps, and Table 2 provides the traffic characteristics information. The maximum speed limits are set as 29 m/s (i.e., 65mph) for the main road and 15.6 m/s (i.e., 35 mph) for the minor road. The four minor intersections in the superstreet system are all signal controlled with a cycle length of 120 s.

#### 3.2. Car-Following Models

**3.2.1. IDM Model.** IDM was developed by Treiber et al. [40]. It is a collision-free model with intuitively measurable

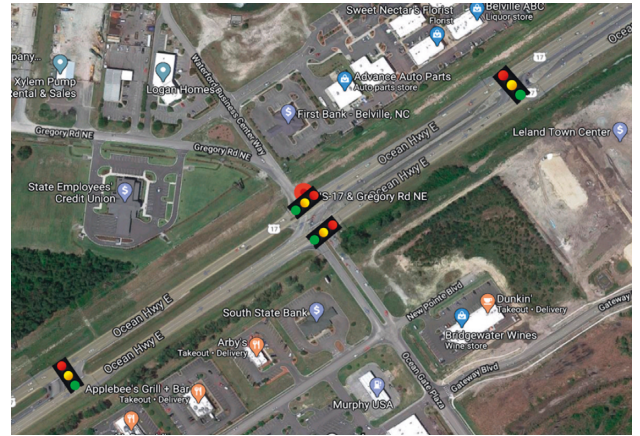


FIGURE 1: Selected superstreet for the case study and signal locations (adapted from the screenshot of google maps).

parameters. Due to these advantages, the IDM has been popularly used in modeling CAVs [1, 41, 42]. The acceleration rate in IDM is a function of the velocity of the subject vehicle, the gap to the preceding vehicle, and the velocity difference to the preceding vehicle, as (1) and (2) show below:

$$a(s, v, \Delta v) = a_m \left( 1 - \left( \frac{v}{v_d} \right)^\alpha - \left( \frac{s^*(v, \Delta v)}{s} \right)^2 \right), \quad (1)$$

$$s^*(v, \Delta v) = s_0 + vT + \frac{v \times \Delta v}{2\sqrt{a_m b}}, \quad (2)$$

TABLE 2: Traffic characteristic information on the superstreet at Leeland, NC.

Approach	Average speed (m/s)	Peak hour demand	Average stops	Travel time (minutes)
EBL	5.99	18	3	2.45
EBR	6.93	20	2	1.38
EBT	5.68	9	2	2.25
NBL	8.00	20	1	1.17
NBR	14.08	71	0	0.64
NBT	14.75	2029	0	0.81
SBL	5.72	321	1	1.26
SBR	14.26	38	0	0.4
SBT	19.58	1637	0	0.58
WBL	8.09	66	2	2
WBR	7.69	345	1	0.89
WBT	5.05	11	2	2.09

where  $a$  indicates the desired acceleration rate;  $a_m$  is the maximum acceleration rate;  $v$  denotes the current speed;  $v_d$  indicates the desired speed (assumed equal to the speed limit in this research);  $v$  represents the speed difference between the subject vehicle and its preceding vehicle;  $\alpha$  means the acceleration exponent, which is set as 4 in this research;  $s$  is the current gap distance between the subject vehicle and its preceding vehicle;  $s_0$  denotes the standing distances (2.5 m);  $T$  represents the desired headway (1s);  $b$  is the maximum deceleration rate.

**3.2.2. W99 Model.** W99 is a microsimulation psychophysical model which has ten parameters available for calibration. These ten parameters are intuitively consistent with human driver behaviors with certain randomness. To ensure that the W99 can represent the local traffic accurately, the ten parameters are calibrated to ensure that the average speeds on each approach in the simulation are matched with the ones that were from the field survey, according to Hummer [13].

Considering the data availability, this research selects the minimal difference between simulated average speeds and observed average speed for each approach as the objective function used in the calibration process. An overall difference within 15% is regarded as acceptable performance.

$$\frac{(\sum_i^N |v_{o,i} * -v_{s,i}|/v_{o,i})}{N}, \quad (3)$$

where  $v_{o,i}$  and  $v_{s,i}$  are the observed and simulated average speed for approach  $i$ , respectively, and  $N$  indicates the total number of approaches.

A genetic algorithm is utilized to minimize the difference between the observed average speeds and simulated average speeds for each approach. GA is a popular and efficient approach to calibrating the car-following model parameters. For brevity, this research skips the introduction of GA. Readers may refer to existing studies of GA calibration for more details [43]. The population size and the maximum number of generations are set as 10 and 20, respectively. The final difference becomes stable at 11%, which is recognized as an acceptable difference. The obtained parameter values from GA are presented in Table 3. The lane changing movement is

controlled by the default car-following model in SUMO, i.e., LC2013 [44].

**3.3. Platooning Schemes.** Vehicle platooning is one of the advanced features of CAVs. It can only be achieved with CAVs that have communication capabilities with other vehicles. Two assumptions were often made with CAVs platooning. One is shorter headways for vehicles inside a defined platoon, and the other is homogenous speeds. With shorter headways and homogenous speeds, the vehicles inside the same platoon can be regarded as a single unit to travel on the road, which can increase the capacity of the roads and also reduce the computational complexity when trajectory planning is involved. This research has also adopted these concepts to fully release the potentiality of CAVs.

**3.3.1. Platoon Formulation and Splitting.** The platoon control system in this research iterates all active vehicles in the simulation environment and checks whether the neighboring vehicles meet the requirements for the platoon formulation. The requirements are that the vehicles

- (1) are in the same lane
- (2) stay within the range of a certain distance
- (3) share the same path

If the requirements above are met, then the system can define such a group of vehicles as a platoon and thus share the same speed with the leading vehicle. However, if any of the vehicles inside the platoon fail to suffice these requirements, then the platoon splits up and switches back to the default car-following model.

There is one more condition guaranteeing platoon splitting. When the platoon is approaching an intersection, the remaining green time  $g_p$  may not be sufficient for all vehicles in a platoon to pass the intersection together, especially when the platoon size is large. Thus, to make the platoon system practical, the vehicles with platooning are assumed to have the knowledge of remaining green time. With the information on the remaining green time  $g_p$ , the platooning system checks whether all vehicles inside a platoon can pass the intersection or not through,



TABLE 3: GA calibrated W99 parameter values.

Parameters	Interpretation	Default values	Calibrated values
CC0	Average standstill distance (meter)	1.4	1.287251
CC1	Headway (seconds)	1.2	1.569918
CC2	Longitudinal oscillation (meters)	8	1.28187
CC3	Start of deceleration process (seconds)	-12	-12.3849
CC4	Minimal closing $\Delta v$ (m/s)	-1.5	-2.398
CC5	Minimal opening $\Delta v$ (m/s)	2.1	0.324976
CC6	Speed dependency of oscillation ( $10^{-4}$ rad/s)	6	4.047425
CC7	Oscillation acceleration-m/s <sup>2</sup>	0.25	0.29111
CC8	Acceleration rate when starting (m/s <sup>2</sup> )	2	4.582238
CC9	Acceleration behavior at 80 km/h (m/s <sup>2</sup> )	1.5	4.261776

$$g_p^w \geq \frac{D_t^i}{v_t^i}, i \in P, \quad (4)$$

where  $g_p^w$  denotes the remaining green time for the platoon  $P$ ,  $D_t^i$  and  $v_t^i$  indicate the remaining distance toward the intersection and the speed of the  $i^{th}$  vehicle inside the platoon  $P$  at the time step  $t$ . In the platoon  $P$ , when  $i^{th}$  the vehicle cannot pass the intersection and the vehicle directly ahead of the  $i^{th}$  vehicle, i.e.,  $i-1^{th}$ , can pass the intersection, then the platoon  $P$  disbands from the  $i-1^{th}$  vehicle. The vehicles after the  $i-1^{th}$  vehicle in the platoon  $P$  would reform a platoon to decelerate together. When the platoons are approaching the intersection, the platooning system checks (4) for each vehicle in the platoons at every time step. In this manner, the platoon system can avoid situations where the platoon runs a red light because of its large platoon size.

**3.3.2. Platooning Behaviors.** The vehicles inside a platoon share the same speed and keep a constant close distance in between. The platoon speed is naturally determined by the leading vehicle's speed. The platoon attempts to set the following vehicles' speeds the same as that of the leading vehicle within acceleration capacity in every time step. If the speed difference between the leading vehicle and the following vehicle exceeds the acceleration/deceleration capacity, the speeds of the following vehicles will execute the boundary speeds to match the leading vehicle's speed as close as possible, as shown in the following:

$$v_t^{\text{following}} = \begin{cases} \max(v_{t-1}^{\text{following}} - a_L, v_{t-1}^{\text{leading}}), & \text{if } v_{\text{leading}} \leq v_{\text{following}}, \\ \min(v_{t-1}^{\text{following}} + a_U, v_{t-1}^{\text{leading}}), & \text{if } v_{\text{leading}} > v_{\text{following}}, \end{cases} \quad (5)$$

where  $v_t^{\text{following}}$  and  $v_{t-1}^{\text{following}}$  indicate the speed of the following vehicle at the time step  $t$  and time step  $t-1$ , respectively, and  $v_{t-1}^{\text{leading}}$  denotes the speed of the leading vehicle at the time step  $t-1$ .

Indeed, in this system, the distance that guarantees a platoon formulation may have an important influence on the performance of the platooning system. Hence, this research also conducts a sensitivity analysis of this parameter. The selection of distance boundaries ranges from 5m to 31m with an increment of 4m. Each distance boundary has 5

simulation runs and each simulation lasts for 900s (15 minutes). This research obtains the traffic delay and fuel consumption to determine the optimal searching distance. Figure 2 provides the average traffic delay and fuel consumption results for each distance boundary. According to Figure 2, it can be observed that both traffic delay and fuel consumption reach relatively low values at a distance of 21m, and thus this research selects 21m as the distance boundary for further analysis.

### 3.4. Trajectory Planning

**3.4.1. Optimal Trajectory Based on Accumulated Absolute Acceleration Rates.** CAVs can plan their trajectories based on the signal information obtained to achieve a certain objective, such as minimizing fuel consumption or traffic delay. The popular approach is to formulate trajectory planning as an optimal control problem whose objective can be a certain traffic performance measure. When the goal is to minimize fuel consumption or emissions, the objective function often takes a nonlinear form and requires nonlinear programming to obtain an optimal solution. Significant computational resources may be required in the real world. A substitute approach to achieving the optimal fuel consumption or emissions benefit is to minimize accumulated absolute acceleration rates along the trajectories, according to [31]. First, a generalized trajectory planning problem of CAVs can be formulated with the objective of minimizing cost  $C$ .

$$\begin{aligned} & \min C(a, v), \\ & \begin{cases} \dot{x}(t) = v(t) \\ \dot{v}(t) = a(t) \end{cases}, \\ & \begin{cases} x(t_0) = 0 \\ v(t_0) = v_0 \end{cases}, \\ & \begin{cases} x(t_f) = D \\ v(t_f) = v_f \end{cases}, \\ & -a_L \leq a(t) \leq a_U, \\ & 0 < v(t) < v_{\max}, \\ & t_0 \leq t \leq t_f, \\ & t_f \text{ fixed.} \end{aligned} \quad (6)$$

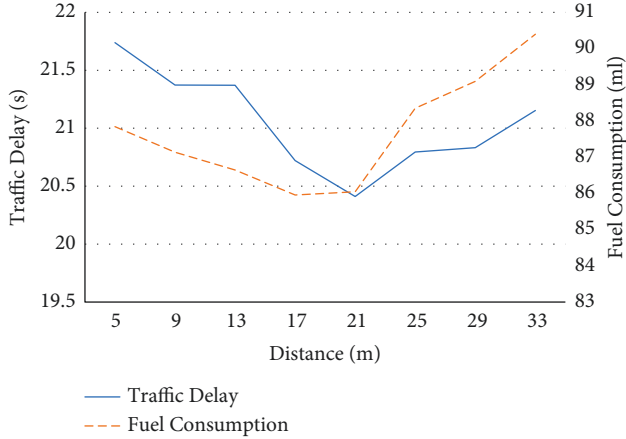


FIGURE 2: Performances of platooning with different values of distance boundaries.

where  $C(a, v)$  represents the cost function,  $x(t)$  and  $v(t)$  are control variables that indicate the traveled distance and instant speed value at the time step  $t$  respectively.  $a(t)$  is the control variable that represents the acceleration rate at time step  $t$ .  $t_0$  and  $t_f$  are the time steps when the CAVs start and finish the trajectory, respectively.  $a_L$  and  $a_U$  represent the absolute values for the maximum deceleration rate and acceleration rates.  $v_{\max}$  indicates the maximum speed (speed limits) while  $v_f$  denotes the final speed when the vehicle arrives at the intersection.  $v_0$  represents the initial speed at which the vehicle enters the communication range between CAVs and signalized intersections.  $D$  is the target distance that the subject vehicle needs to travel, which often is the distance between the vehicle and the intersection. The fuel consumption or emission is known to be significantly related to the acceleration rates. [31] developed a trajectory planning strategy to minimize fuel consumption based on Pontryagin's Minimum Principle (PMP). Through analysis of PMP, a generalized solution can be achieved with the objective of minimizing the accumulated absolute acceleration rates along the trajectory, which is as follows:

$$\min C = \int_{t_0}^{t_f} |a(t)| dt. \quad (7)$$

The solution to the optimal trajectory generally results in a three-segment trajectory, in which vehicles remain at a constant speed at the second segment. The first and the third segment have a constant either maximum acceleration or deceleration rate according to the relationships between the [31]initial speed and final speed, as Figure 3(a) shows. Figure 3(b) provides an example comparison of when CAVs are enabled with and without such trajectory planning feature.

The transition time steps  $t_1$  and  $t_2$  can be determined given the following equations in the deceleration case ( $v_0 > v_f$ ) and acceleration case ( $v_0 < v_f$ ), respectively, where  $v_c$  indicates the constant speed in the second segment and the other variables are defined earlier.

$$\frac{v_0 + v_c}{2} * t_1 + v_c * (t_2 - t_1) + \frac{v_f + v_c}{2} * (t_f - t_2) = D, \quad (8)$$

$$v_c = \begin{cases} v_0 - a_L * t_1 = v_f + a_L(t_f - t_2), v_0 > v_f, \\ v_0 + a_U * t_1 = v_f - a_U(t_f - t_2), v_0 < v_f. \end{cases}$$

Additionally, one can obtain the lower and upper travel time boundary to guarantee that a feasible solution will be obtained as shown below:

$$v_0 > v_f \begin{cases} t_L = \frac{D}{v_0} + \frac{(v_0 - v_f)^2}{2 * v_0 * a_L}, \\ t_U = \frac{D}{v_f} - \frac{(v_0 - v_f)^2}{2 * v_f * a_L}, \end{cases} \quad (9)$$

$$v_0 < v_f \begin{cases} t_L = \frac{D}{v_f} + \frac{(v_0 - v_f)^2}{2 * v_f * a_U}, \\ t_U = \frac{D}{v_0} - \frac{(v_0 - v_f)^2}{2 * v_0 * a_U}. \end{cases} \quad (10)$$

Notably, a feasible three-segment trajectory solution only exists when the vehicle arrival time  $t_f$  is strictly within the boundary of  $t_L$  and  $t_U$ , i.e.,

$$t_L < t_f < t_U. \quad (11)$$

When  $t_f = t_L$  or  $t_f = t_U$ , the three-segment trajectory solution collapses into the two-segment trajectory. The lower/upper-time boundaries indicate two-segment trajectories in acceleration and deceleration, respectively, as shown in Figure 4.

In a deceleration scenario, the lower boundary indicates that the vehicle keeps its current speed in the first segment and then decelerates to its final speed in the second segment. The upper boundary indicates that the vehicle first decelerates to the target final speed, then keeps the target final speed until it arrives at the intersection. On the other hand, in an acceleration scenario, the lower boundary indicates that the vehicle first accelerates the final speed  $v_f$  and then cruises at the target speed until arriving at the intersection. When the final speed  $v_f$  is equal to the maximum speed  $v_{\max}$  such trajectory type can yield the minimum travel time  $t_{\text{minimum}}$  and thus is referred to as the minimum travel time trajectory. The upper boundary in an acceleration scenario means that the vehicle first keeps its initial speed and then accelerates to its target speed. Intuitively, when the travel time is strictly within the lower- and upper-time boundaries, then an optimal three-segment trajectory exists. When the travel time is equal to one of the two boundary values, then a two-segment trajectory introduced above can be applied. Nevertheless, when travel time exceeds the boundary, then no feasible solution exists with the given distance,

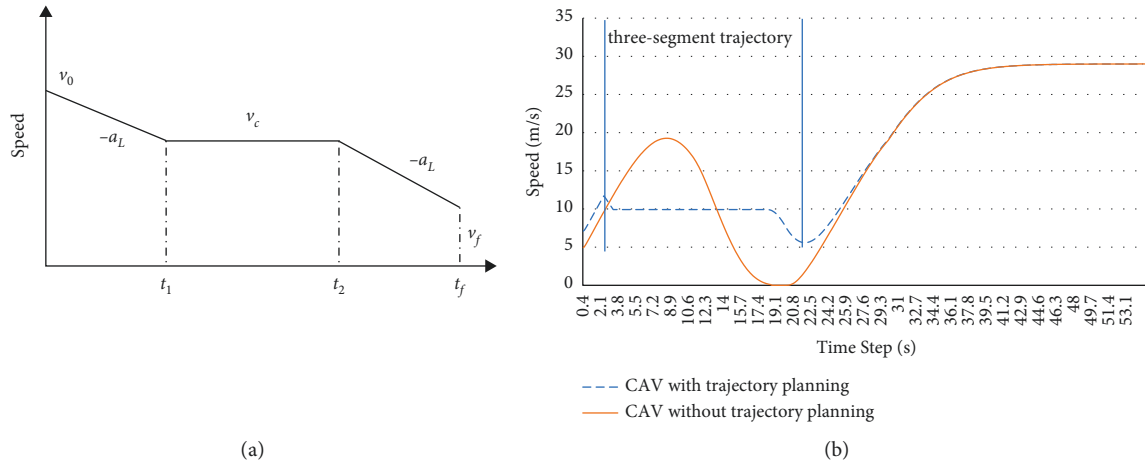


FIGURE 3: A general optimal trajectory for the deceleration scenario. (a) Theoretical three-segment trajectory in deceleration case (revised from (b) Three-segment trajectory in simulation.

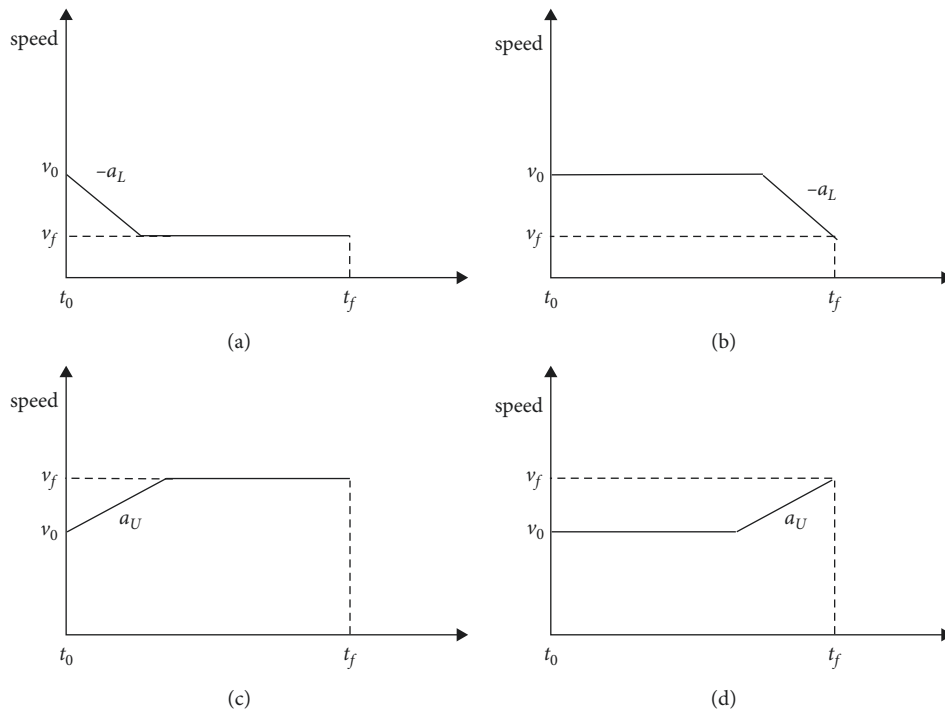


FIGURE 4: The two-segment trajectory when the travel time is equal to the boundary values. (a)  $t_f = t_U$  and  $v_0 > v_f$ . (b)  $t_f = t_L$  and  $v_0 > v_f$ . (c)  $t_f = t_L$  and  $v_0 < v_f$ . (d)  $t_f = t_U$  and  $v_0 < v_f$ .

acceleration rate, and initial speeds. This reflects real-world scenarios. For example, a vehicle may not be able to decelerate to a speed of zero if the remaining distance to the intersection is too short or the initial speed is too high.

Demonstrated that this trajectory planning strategy could successfully [31] reduce traffic delay and fuel consumption in a standard isolated conventional intersection with a joint adaptive signal optimization algorithm. With the adaptive signal control, Equation (11) can stand for most cases and the vehicle can avoid stops under certain traffic conditions. Nevertheless, this strategy cannot be directly

transferred to a fixed signal-controlled intersection. In a fixed signal-controlled intersection, the final travel time  $t_f$  is largely dependent on the initiation time or remaining time of the target green phase in a fixed signal timing plan, where vehicles cannot avoid stopping entirely. To apply this trajectory planning scheme in a fixed signal-controlled intersection, this research also considers a constant deceleration trajectory when (11) cannot be sufficed. For a constant deceleration trajectory, the vehicle will keep a constant deceleration rate until it arrives at the intersection with a speed of 0, as shown in Figure 5. The deceleration rate  $a_{dec}$

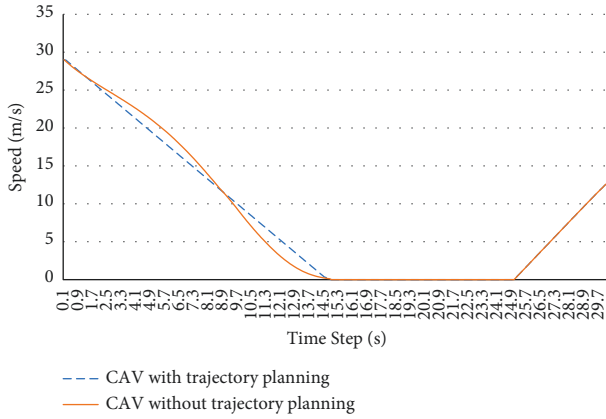


FIGURE 5: Constant deceleration trajectory.

can be easily obtained through the basic kinetic law, which is described by (11).

$$a_{dec} = \frac{v_0}{2 * D/v_0}. \quad (12)$$

Based on the signal status and the next signal switch time  $t_{switch}$ , the vehicle can choose different speed trajectories as introduced above.

(1) *Red Signal.* When the upcoming signal status for the subject vehicle is red, the signal switch time  $t_{switch}$  indicates the initiation of green time. The lower time boundary obtained through (10) is equal to the minimum travel time  $t_{minimum}$  when the given final speed  $v_f = v_{max}$ . If the switch time  $t_{switch}$  is less than or equal to the  $t_{minimum}$ , then the vehicle can meet a green signal with a two-segment trajectory as shown in Figure 6 to achieve minimal traffic delay.

If the switch time is greater than the minimum travel time, i.e.,  $t_{switch} \geq t_{minimum}$ , then the vehicle with a minimum travel time trajectory will meet a red signal. In this situation, it is assumed that  $t_f = t_{switch}$ . From (9) and (10), one may obtain  $t_L$  and  $t_U$  given a final speed  $v_f$ . Hence, researchers may simply enumerate all possible final speeds  $[0, v_{max})$  to obtain a feasible speed candidate list  $\mathbf{V}_f$  so that (12) stands.

$$t_L < t_{switch} < t_U. \quad (13)$$

This research selects the  $\max(\mathbf{V}_f)$  so that the subject vehicle can travel through the intersection with maximum final speed to minimize the traffic delay, where the max function returns the maximum value among the feasible final speed list  $\mathbf{V}_f$ .

(2) *Green Signal.* If the ahead signal status is green, then  $t_{signalswitch}$  indicates the remaining green time for the subject vehicle. This research mainly considers two cases based on the relationship between signal switch time  $t_{signalswitch}$  and minimum travel time  $t_{minimum}$  of the subject vehicle.

*Case 1.* When the subject vehicle can traverse through the intersection with minimum travel time  $t_{minimum}$  (i.e.,  $t_{signalswitch} \geq t_{minimum}$ ), then the vehicle may accelerate its maximum speed to pass the intersection to achieve the

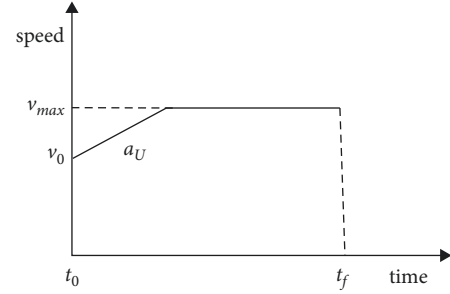


FIGURE 6: Speed trajectory with minimum travel time.

minimal traffic delay. However, this strategy may potentially increase the average fuel consumption as the fuel consumption is closely related to the acceleration rate. In some circumstances, if the  $t_{signalswitch} \geq t_{currentspeed}$ , where  $t_{currentspeed}$  is the travel time to the intersection when the vehicle keeps its current speed, then the decision-makers who assign a higher priority to fuel consumption may let the vehicle keep its current speed to avoid increasing fuel consumption with acceptable compromise on the traffic delay.

*Case 2.*  $t_{signalswitch} \leq t_{minimum}$  means the subject vehicle cannot arrive at the intersection within the given remaining green time even if the vehicle accelerates to maximum speed. In such a situation, a constant deceleration trajectory introduced above may be executed. The subject vehicle may need to check whether the vehicle can meet the second green with a given final speed within  $[0, v_{max})$  when the distance  $D$  is large.

*3.4.2. Encountering Preceding Vehicles during Trajectory Planning.* In the real world, the vehicles may have close preceding vehicles on the road, and following the predetermined trajectories may lead to collisions with the preceding vehicles. Therefore, to avoid these collisions in this research, when a vehicle has preceding vehicles that are within a 3s headway, the vehicle will stop executing the planned trajectory and switch to the predefined car-following model, which is the IDM model in this research. Note that the system constantly checks each vehicle's distance to the preceding vehicles at each time step. When the distance to the preceding vehicle is greater than 3s and there is an upcoming signalized intersection, then the system will plan the vehicle trajectory again for the subject vehicle to follow. With this function, the vehicles following the planned trajectory can successfully avoid collision with not only the close preceding vehicles but also the queueing vehicles in front of the intersection because of the red signal.

*3.5. Simulation Scenarios and Relevant Settings.* An equivalent conventional intersection with the same road segment length, lane configuration, and maximum speed is designed in the simulation platform. The cycle length is also set the same as the superstreet in the real world, i.e., 120s, to make a fair comparison. The green splits for each approach are determined



by their volume ratios. To account for different traffic conditions, this research tests four different traffic scales including 25%, 50%, 75%, and 100% of peak hour traffic volumes from Table 2. Furthermore, a market penetration analysis is conducted on the 100% peak hour traffic volumes. 25%, 50%, and 75% of CAV market penetration rates are considered in the simulation. Every scenario is run five times with different random seeds to account for the randomness. To make the system more robust and increase calculation accuracy, the simulation resolution is set as 10HZ, which means the simulation runs 10 time steps every second. Once the vehicle enters the roadway network, the vehicle is assumed to enter the Vehicle-to-Infrastructure (V2I) communication range, which is reasonable since the selected superstreet has a rather short road segment length in all approaches before the traffic signals (less than 300 m). Average traffic delay (delay per vehicle) and fuel consumption (fuel consumption per vehicle) are the performance indicators that are used for this research. Traffic delay is measured by the ideal travel time (free-flow speed without any stop) minus actual travel time. Fuel consumption is measured by the default emission model from SUMO, i.e., HBEFT.3 [45]. The maximum acceleration rates and deceleration rates for IDM are set as  $2.5 \text{ m/s}^2$ . Considering drivers' comfort, the maximum acceleration rate and deceleration rate in CAV trajectory planning are  $2 \text{ m/s}^2$ .

## 4. Results and Discussion

### 4.1. The Performance of CAVs in Conventional Intersections

**4.1.1. Traffic Delay.** To provide an initial understanding of the performance of CAVs, this research first obtains the simulation results of CAVs from the equivalent conventional intersection. The traffic delay results are presented in Figure 7. From Figure 7, it can be observed that the developed platooning, trajectory planning, and platooning-based trajectory planning can reduce the traffic delay in most scenarios. The exception is CAVs with platooning at 25%. When CAVs are enabled with platooning, the speed of the following vehicles is influenced by the leading vehicle in the same platoon and may not be able to achieve their maximum speeds even in light traffic volume. This may potentially explain that no benefit is gained for platooning in the traffic demand of 25% and 50% peak hour traffic volume scenarios. The traffic delay improvements for CAV with platooning increase as the traffic demand increases.

Trajectory planning can reduce traffic delay to a larger extent in light traffic volume scenarios, and the improvement magnitudes shrink as the traffic volumes increases. These results can be explained by the trajectory planning modeling framework. As mentioned in the methodology section, to avoid collisions with preceding vehicles and queueing vehicles in front of the intersection, CAVs with trajectory planning may switch to the default car-following model frequently in high traffic demand scenarios. For CAV with platooning-based trajectory planning, the traffic delays share a similar trend as the ones from CAV with platooning. Notably, platooning-based trajectory planning also successfully reduces the traffic delay in low traffic demand scenarios.

**4.1.2. Fuel Consumption.** From Figure 8, it can be observed that platooning could provide larger benefits in terms of fuel consumption in high traffic volume scenarios. The improvement magnitudes are also consistent with existing studies on platooning [46]. The proposed trajectory planning framework reduces the average fuel consumption to a certain extent in low traffic volume scenarios. However, the fuel consumption benefits from trajectory planning are less significant compared to platooning. In addition, the trajectory planning framework may produce adverse effects on fuel consumption in high traffic volume scenarios, as observed in 100% peak hour traffic volume scenarios. In high traffic volume scenarios, CAVs with trajectory planning capability change to the car-following model frequently because of the presence of preceding vehicles, which may produce speed fluctuations and higher fuel consumption. CAV with platooning-based trajectory planning produces the optimal fuel consumption results in most traffic demand levels.

**4.2. Comparison between CAVs and HDVs with Calibrated W99.** This research first examines the performance of the calibrated W99 model, IDM model, IDM with platooning, IDM with trajectory planning, and IDM with platooning-based trajectory under 100% peak hour traffic volume, respectively.

Although it is expected that CAVs outperform HDVs, it may not be necessarily always true in the real world. For instance, when the vehicle travels through a congested intersection, HDVs are likely to have shorter headways and practice emergency deceleration or acceleration to achieve minimal travel time or avoid collisions, while CAVs cannot exceed the predetermined boundary of safe headway and acceleration rates. According to Figure 9, the results from calibrated W99 and IDM prove this assumption since they have similar average delays and fuel consumption.

However, when CAVs are enabled with platooning and trajectory planning, the CAVs may be superior to HDVs. For the proposed platooning model, compared to the IDM model, the traffic delay decreases from 23.42 to 20.49 (around 13%), while the fuel consumption decreases from 95.79 to 85.87 (around 10% reduction). Since HDVs with calibrated W99 have similar traffic delay and fuel consumption, similar improvements can be found when comparing CAV with platooning against HDVs with calibrated W99. Table 4 presents the comparison results between CAVs with different features and HDVs with calibrated W99.

The outstanding performance of platooning performances may be related to the large traffic volume in this scenario. On the other hand, IDM with trajectory planning has few benefits in terms of both traffic delay and fuel consumption compared to IDM only. As described in the previous section, CAVs will change into the car-following model when they detect vehicles that are within a 3s headway. In a congested traffic condition such as 100% peak hour traffic volume, the advantages of trajectory planning are significantly compromised. As for CAVs with platooning-based trajectory planning, the traffic delay decreases and reaches the lowest traffic delay (19.80s) among all scenarios,

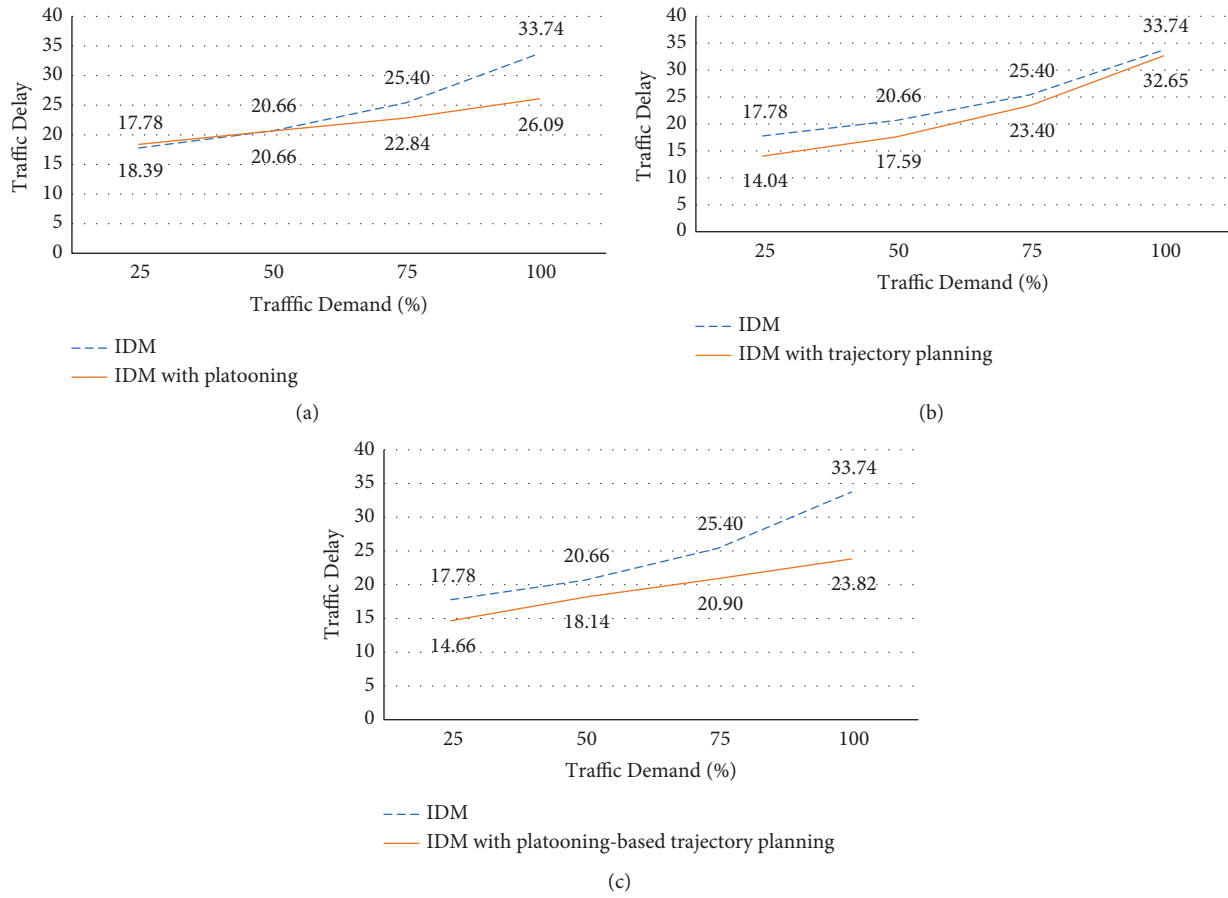


FIGURE 7: Average traffic delay(s) of CAVs in the equivalent conventional intersection. (a) Average traffic delay for IDM and IDM with platooning (b) Average traffic delay for IDM and IDM with trajectory planning. (c) Average traffic delay for IDM and IDM with platooning-based trajectory planning.

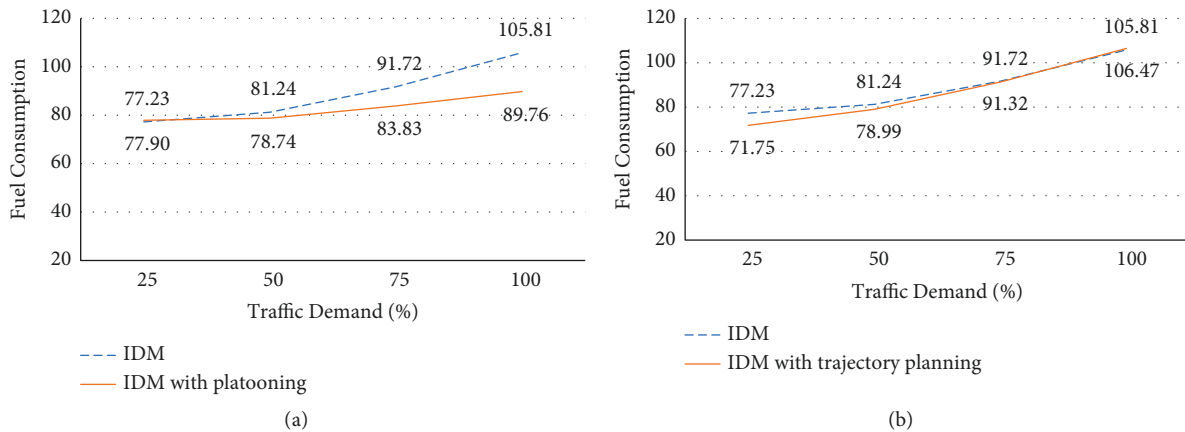


FIGURE 8: Continued.

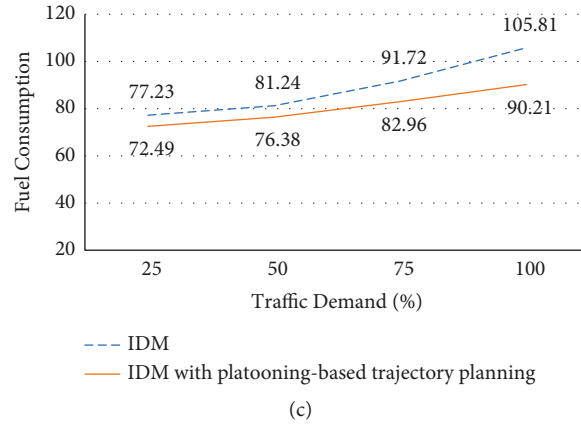


FIGURE 8: Average fuel consumption(ml) of CAVs in the equivalent conventional intersection. (a) Average fuel consumption for IDM and IDM with platooning. (b) Average fuel consumption for IDM and IDM with trajectory planning. (c) Average fuel consumption for IDM and IDM with platooning-based trajectory planning.

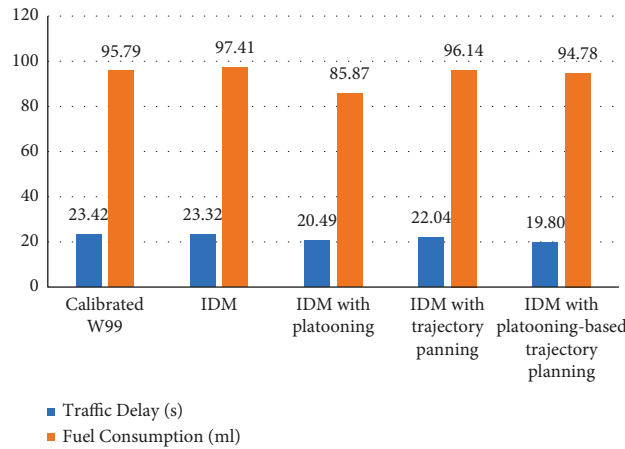


FIGURE 9: Traffic performances with different scenarios.

TABLE 4: CAV performances compared to HDVs with calibrated W99.

	TD <sup>1</sup>	Improvement <sup>2</sup> (%)	FC <sup>3</sup>	Improvement <sup>4</sup>
IDM	23.32	0	97.41	-2%
IDM with platooning	20.49	13	85.87	10%
IDM with trajectory planning	22.04	6	96.14	0%
IDM with platooning-based trajectory planning	19.80	15	94.78	1%

<sup>1</sup> average traffic delay in seconds; <sup>2</sup> benchmark is 23.42; <sup>3</sup> average fuel consumption in milliliter; <sup>4</sup> benchmark is 95.79.

while the fuel consumption is lower compared to CAVs with trajectory planning but higher compared to CAVs with platooning. CAVs with platooning and trajectory planning, when vehicles are close to each other, form a platoon so that trajectory planning can be executed, which explains the greater traffic delay reduction in CAVs with platooning-based trajectory planning. The fuel consumption of platooning-based trajectory planning is higher than the ones of platooning but lower than the ones of trajectory planning.

### 4.3. The Performances of CAVs in Superstreets

4.3.1. *Traffic Delay.* Figure 10 presents the average traffic delay when CAVs are enabled with platooning, trajectory planning, and platooning-based trajectory planning. CAVs with platooning have similar performances as they did in the equivalent conventional intersection. When the traffic scale is at 25% peak hour traffic volume, the CAVs with platooning fails to reduce the average traffic delay. Nevertheless,

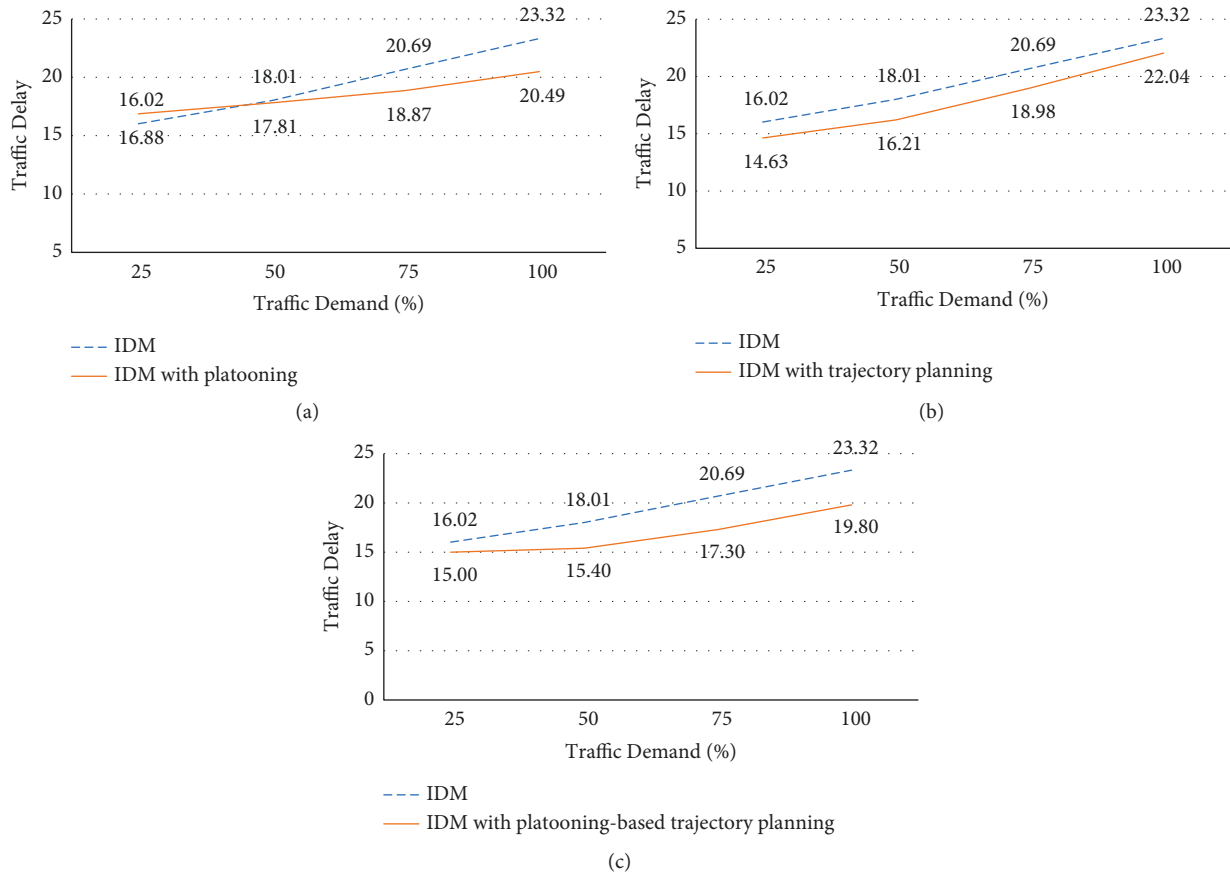


FIGURE 10: Average traffic delay(s) of CAVs in the superstreet. (a) Average traffic delay for IDM and IDM with platooning. (b) Average traffic delay for IDM and IDM with trajectory planning. (c) Average traffic delay for IDM and IDM with platooning-based trajectory planning.

when the traffic demand is greater or equal to 50% of peak hour traffic volume, the CAVs start to reduce the traffic delay in the superstreet.

As for trajectory planning, the reductions of traffic delay in different demands are relatively constant compared to the ones in the conventional intersection. In superstreet, the road capacity often is larger than the equivalent conventional intersection. Therefore, CAVs might not have to switch to the car-following model frequently as they did in the equivalent conventional intersection in 100% peak hour traffic volume demand, which explains the relevant constant traffic delay reduction.

CAVs with platooning-based trajectory planning still produce minimal traffic delays in nearly all demand levels (except for 25% peak hour traffic demand). The general trend of traffic delays is similar to that in platooning scenarios as in the equivalent conventional intersection.

**4.3.2. Fuel Consumption.** Figure 11 presents the fuel consumption of CAVs in the superstreet. Platooning yields similar fuel consumption trends as it did in the traffic delay results. Nevertheless, CAVs with trajectory planning produce higher average fuel consumption, especially in the lower traffic demand scenarios. The increased average fuel

consumption is potentially attributed to two reasons: (1) the acceleration behavior of CAVs with trajectory planning in order to catch the remaining green or initiation green time; (2) CAVs with trajectory planning may stop at the second consecutive intersection after passing the first intersection with acceleration in the superstreet system. In high traffic volume scenario, the adverse effects of fuel consumption are alleviated since CAVs with trajectory planning do not have much freedom of accelerating before the intersection. This result demonstrates the necessity of incorporating two consecutive signal information in designing a trajectory planning framework when two signals are closely spaced. The adverse effects on fuel consumption are alleviated when CAVs are enabled with platooning-based trajectory planning.

**4.3.3. CAVs with Different Market Penetration Rates.** The dominance of CAVs on the road is a gradual process in which technology, political and legal challenges continuously remain. The policymakers may be interested in the performances of CAVs with different levels of market penetration rates. Therefore, this research also conducts a market penetration analysis where HDVs controlled by calibrated W99 and CAVs controlled by IDM with



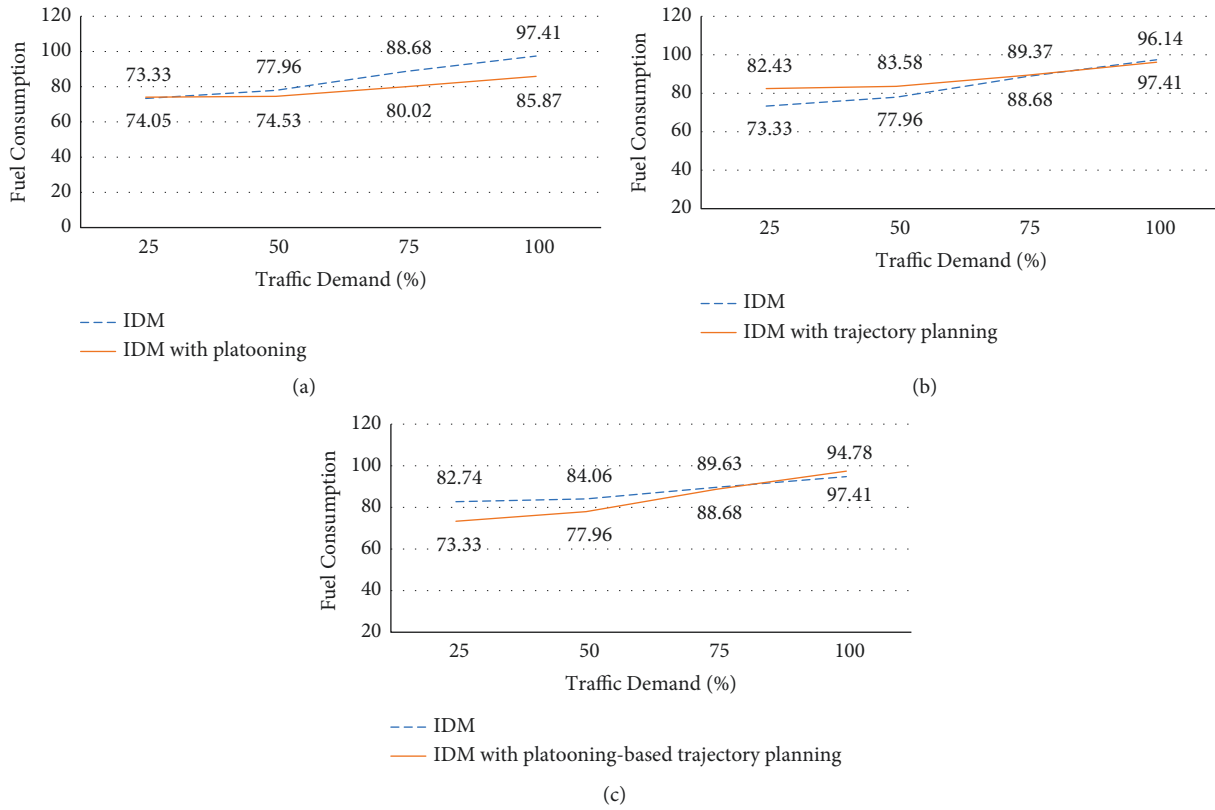


FIGURE 11: Average fuel consumption (ml) of CAVs in the superstreet. (a) Average fuel consumption for IDM and IDM with platooning. (b) Average fuel consumption for IDM and IDM with trajectory planning. (c) Average fuel consumption for IDM and IDM with platooning-based trajectory planning.

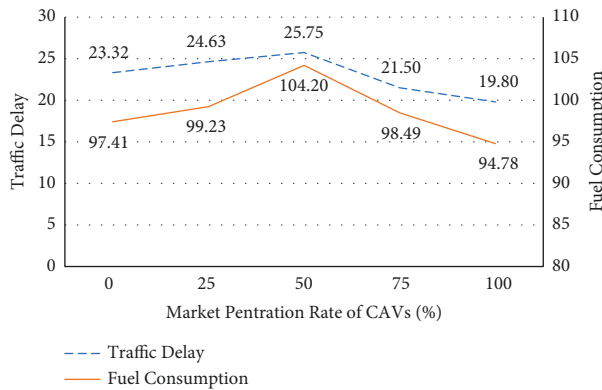


FIGURE 12: Analysis for different CAV market penetration rates.

platooning-based trajectory planning coexist. 25%, 50%, and 75% CAV market penetration rates are tested under 100% peak hour traffic volume. When CAVs follow HDVs, CAVs are often assumed to have larger headways [47]. Therefore, when CAVs follow HDVs, the CAV headway is set the same as HDVs, i.e., 1.6s. Figure 12 provides the results of the market penetration analysis. Based on Figure 12, it can be observed that traffic delay starts to fall at the market penetration of 75% CAVs, where the fuel consumption is similar to that of 0% CAV. The fuel consumption and traffic delay are highest when the market penetration rate of CAVs is at

the 50% level. Overall, the more mixed the vehicle types are (i.e., equal market penetration rate of CAVs and HDVs), the worse the traffic performance is.

4.4. A Comparison between Conventional Intersection and Superstreet. Figures 13 and 14 compare the average traffic delay and fuel consumption of CAVs in the equivalent conventional intersection and superstreet, respectively. Based on Figure 13, with IDM vehicles, the superstreet can consistently outperform the equivalent conventional

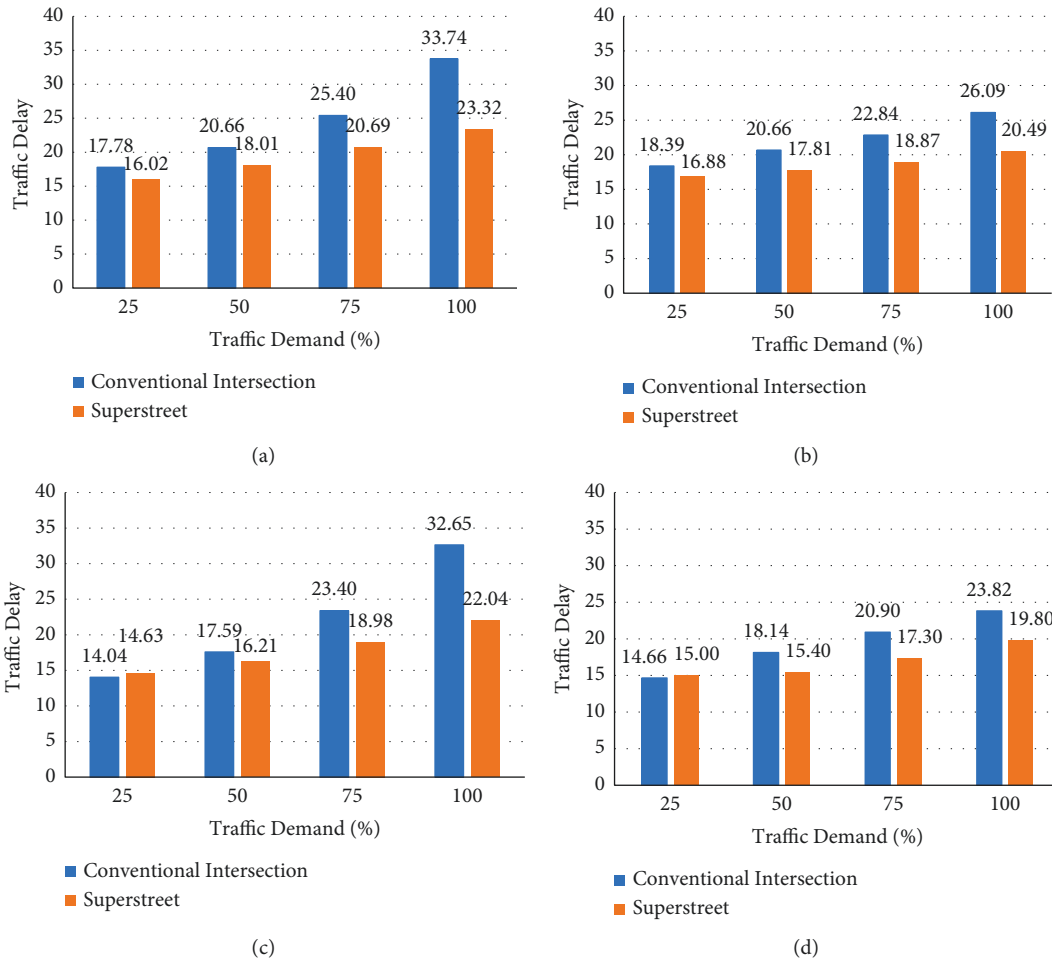


FIGURE 13: Average traffic delay(s) comparison of CAVs between the conventional intersection and superstreet. (a) IDM. (b) IDM with platooning. (c) IDM with trajectory planning. (d) IDM with platooning-based trajectory planning.

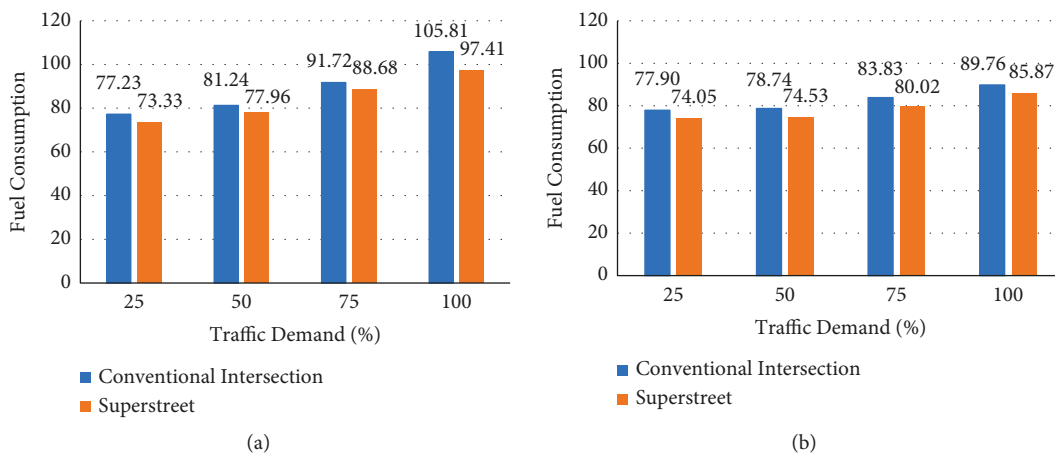


FIGURE 14: Continued.

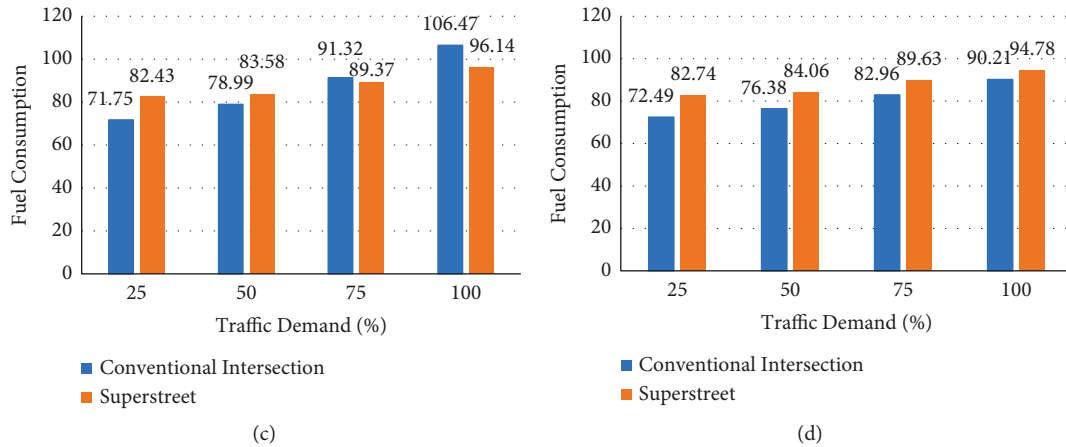


FIGURE 14: Average fuel consumption(ml) comparison of CAVs between the conventional intersection and superstreet. (a) IDM. (b) IDM with platooning. (c) IDM with trajectory planning. (d) IDM with platooning-based trajectory planning.

TABLE 5: Average traffic delay improvement magnitudes of superstreet compared to the equivalent conventional intersection with different CAV Features.

CAV features	Peak demand scale			
	25%	50%	75%	100%
IDM	10%	13%	19%	31%
IDM with platooning	8%	14%	17%	21%
IDM with trajectory planning	-4%	8%	19%	32%
IDM with platooning-based trajectory planning	-2%	15%	17%	17%

TABLE 6: Average fuel consumption improvement magnitudes of superstreet compared to the equivalent conventional intersection with different CAV Features.

CAV features	Peak demand scale			
	25%	50%	75%	100%
IDM	5%	4%	3%	8%
IDM with platooning	5%	5%	5%	4%
IDM with trajectory planning	-15%	-6%	2%	10%
IDM with platooning-based trajectory planning	-14%	-10%	-8%	-5%

intersection regarding average traffic delay. However, it could also be observed that the average traffic delay differences between the conventional intersection and superstreet are reduced in platooning and platooning-based trajectory planning scenarios compared to CAVs controlled by IDM only.

As for fuel consumption, Figure 14 shows that the average fuel consumptions of CAVs with trajectory planning are higher when they are in the superstreet under 25% and 50% peak hour traffic volume. When CAVs are enabled with platooning-based trajectory planning, they have higher average fuel consumption on all demand levels in the superstreet. As explained in the previous section, this may potentially result from the lack of consideration of two closely spaced signalized intersections when developing the trajectory planning control framework. Tables 5 and 6 provide improvement magnitudes of superstreet compared to the conventional intersection in terms of the average traffic delay and fuel consumption, respectively.

## 5. Conclusions

This research investigated the performances of CAVs and HDVs in the environments of the superstreet and conventional intersection. CAVs were modeled with the IDM car-following model, while HDVs were modeled with the W99 car-following model. A real-world superstreet situated in Leeland, NC, was replicated in the simulation platform to test the performances of CAVs and HDVs under different traffic conditions. In addition, to fully examine the potentiality of CAVs, a simple platooning scheme and trajectory planning strategy were developed for CAVs, respectively. In this research, the W99 model was calibrated with GA so that the W99 model can better represent the local drivers' behaviors. Different traffic demands and market penetration rates were taken into consideration in the designed scenarios.

The simulation results indicated that without platooning and trajectory planning, CAV modeled by IDM did not have significant improvement compared to HDVs modeled by

W99. The developed platooning strategy can successfully reduce the traffic delay and fuel consumption at relatively high traffic demand scenarios (50%, 75%, and 100% peak hour volume) in both the superstreet and the conventional intersection. Trajectory planning could reduce the traffic delay in both superstreet and conventional intersection environments but with different impacts on fuel consumption. CAVs with trajectory planning produced higher fuel consumption in the superstreet in the lower traffic demand scenarios, especially in traffic demand 25% and 50% of peak hour traffic volume. A potential reason is that CAVs which accelerate to pass the first intersection may fail to pass the consecutive second intersection in the environment of superstreet. In the market penetration rate analysis of CAVs, it was found that the mixed traffic environment can compromise the benefit when the CAVs market penetration rates were at 25% and 50% peak hour traffic volume. CAVs have better performances when the market penetration rate is about 75% and above.

This research also compared the traffic performances of CAVs in the conventional intersection and superstreet. A notable finding was that the proposed trajectory planning control strategy can successfully reduce the average traffic delay without increasing the average fuel consumption in the conventional intersection. This was different from superstreet where CAVs enabled with trajectory planning increase the fuel consumption. This demonstrated the efficiency of the proposed trajectory planning strategy in an isolated intersection. However, this result also indicated that the trajectory planning without considering special features of two closely spaced signalized intersections may suffer adverse effects on fuel consumption. Overall, the improvement magnitude of platooning and trajectory planning was larger in the conventional intersection.

Based on these research findings, the future research directions could be the adaptive signal control strategy that takes arrival information on CAVs into consideration, which may reduce the adverse effects of trajectory planning on fuel consumption identified in this research. Also, a more sophisticated trajectory planning algorithm that takes into account two consecutive signalized intersections can be developed.

## Data Availability

All data, models, or codes that support the findings of this study are available from the corresponding author upon reasonable request.

## Conflicts of Interest

The authors declare that they have no conflicts of interest.

## Acknowledgments

The authors want to express their deepest gratitude for the financial support by the United States Department of Transportation, University Transportation Center through the Center for Advanced Multimodal Mobility Solutions and

Education (CAMMSE) at the University of North Carolina at Charlotte (Grant no. 69A3551747133).

## References

- [1] P. Liu and W. D. Fan, "Exploring the impact of connected and autonomous vehicles on freeway capacity using a revised Intelligent Driver Model," *Transportation Planning and Technology*, vol. 43, no. 3, pp. 279–292, 2020.
- [2] X. Guo, Y. Peng, S. Ashraf, and M. W. Burris, "Performance analyses of information-based managed lane choice decisions in a connected vehicle environment," *Transportation Research Record: Journal of the Transportation Research Board*, vol. 2674, no. 11, pp. 120–133, 2020.
- [3] J. Guo, S. Cheng, and Y. Liu, "Merging and diverging impact on mixed traffic of regular and autonomous vehicles," *IEEE Transactions on Intelligent Transportation Systems*, vol. 22, no. 3, pp. 1639–1649, 2021.
- [4] R. Mohebifard and A. Hajbabaie, "Connected automated vehicle control in single lane roundabouts," *Transportation Research Part C: Emerging Technologies*, vol. 131, Article ID 103308, 2021.
- [5] R. Mohebifard and A. Hajbabaie, "Trajectory Control in Roundabouts with a Mixed Fleet of Automated and Human-driven Vehicles," *Computer-Aided Civil and Infrastructure Engineering*, 2021.
- [6] H. Jiang, J. Hu, S. An, M. Wang, and B. B. Park, "Eco approaching at an isolated signalized intersection under partially connected and automated vehicles environment," *Transportation Research Part C: Emerging Technologies*, vol. 79, pp. 290–307, 2017.
- [7] X. Han, R. Ma, and H. M. Zhang, "Energy-aware trajectory optimization of CAV platoons through a signalized intersection," *Transportation Research Part C: Emerging Technologies*, vol. 118, Article ID 102652, 2020.
- [8] Z. Zhong, E. E. Lee, M. Nejad, and J. Lee, "Influence of CAV clustering strategies on mixed traffic flow characteristics: an analysis of vehicle trajectory data," *Transportation Research Part C: Emerging Technologies*, vol. 115, Article ID 102611, 2020.
- [9] C. Mu, L. Du, and X. Zhao, "Event triggered rolling horizon based systematical trajectory planning for merging platoons at mainline-ramp intersection," *Transportation Research Part C: Emerging Technologies*, vol. 125, Article ID 103006, 2021.
- [10] J. Hummer, B. Ray, A. Daleiden, P. Jenior, and J. Knudsen, "Restricted Crossing U-Turn: Informational Guide," Report\No. FHWA-SA-14-070, Federal Highway Administration Office of Safety, Washington, DC, USA, 2014.
- [11] R. L. Haley, S. E. Ott, J. E. Hummer, R. S. Foyle, C. M. Cunningham, and B. J. Schroeder, "Operational effects of signalized superstreets in North Carolina," *Transportation Research Record: Journal of the Transportation Research Board*, vol. 2223, no. 1, pp. 72–79, 2011.
- [12] H. H. Naghawi, "Analyzing delay and queue length using microscopic simulation for the unconventional intersection design Superstreet," *Journal of the South African Institution of Civil Engineering= Joernaal van die Suid-Afrikaanse Instituut van Siviele Ingenieurswese*, vol. 56, no. 1, pp. 100–107, 2014.
- [13] J. E. Hummer, R. L. Haley, S. E. Ott, R. S. Foyle, and C. M. Cunningham, "Superstreet Benefits and Capacities," Report\No. FHWA/NC/2009-06, Institute for Transportation Research and Education, Raleigh, NC, USA, 2010.
- [14] L. Xu, X. Yang, and G.-L. Chang, "Computing the minimal U-turn offset for an unsignalized superstreet," *Transportation*



- Research Record: Journal of the Transportation Research Board*, vol. 2618, no. 1, pp. 48–57, 2017.
- [15] L. Xu, X. Yang, and G.-L. Chang, “Two-stage model for optimizing traffic signal control plans of signalized Superstreet,” *Transportmetrica: Transport Science*, vol. 15, no. 2, pp. 993–1018, 2019.
  - [16] Y. Qin, H. Wang, and B. Ran, “Stability analysis of connected and automated vehicles to reduce fuel consumption and emissions,” *Journal of Transportation Engineering, Part A: Systems*, vol. 144, no. 11, Article ID 04018068, 2018.
  - [17] J. Rios-Torres and A. A. Malikopoulos, “Impact of partial penetrations of connected and automated vehicles on fuel consumption and traffic flow,” *IEEE Transactions on Intelligent Vehicles*, vol. 3, no. 4, pp. 453–462, 2018.
  - [18] A. Adebisi, Y. Liu, B. Schroeder et al., “Developing highway capacity manual capacity adjustment factors for connected and automated traffic on freeway segments,” *Transportation Research Record: Journal of the Transportation Research Board*, vol. 2674, no. 10, pp. 401–415, 2020.
  - [19] S. Chityala, J. O. Sobanjo, E. Erman Ozguven, T. Sando, and R. Twumasi-Boakye, “Driver behavior at a freeway merge to mixed traffic of conventional and connected autonomous vehicles,” *Transportation Research Record: Journal of the Transportation Research Board*, vol. 2674, no. 11, pp. 867–874, 2020.
  - [20] X. Hu and J. Sun, “Trajectory optimization of connected and autonomous vehicles at a multilane freeway merging area,” *Transportation Research Part C: Emerging Technologies*, vol. 101, pp. 111–125, 2019.
  - [21] M. Pourmehr, P. Emami, M. Martin-Gasulla, J. Wilson, L. Eleftheriadou, and S. Ranka, “Signalized intersection performance with automated and conventional vehicles: a comparative study,” *Journal of Transportation Engineering, Part A: Systems*, vol. 146, no. 9, Article ID 04020089, 2020.
  - [22] Y. Guo, J. Ma, C. Xiong, X. Li, F. Zhou, and W. Hao, “Joint optimization of vehicle trajectories and intersection controllers with connected automated vehicles: combined dynamic programming and shooting heuristic approach,” *Transportation Research Part C: Emerging Technologies*, vol. 98, pp. 54–72, 2019.
  - [23] P. Li and X. Zhou, “Recasting and optimizing intersection automation as a connected-and-automated-vehicle (CAV) scheduling problem: a sequential branch-and-bound search approach in phase-time-traffic hypernetwork,” *Transportation Research Part B: Methodological*, vol. 105, pp. 479–506, 2017.
  - [24] F. Zhou, X. Li, and J. Ma, “Parsimonious shooting heuristic for trajectory design of connected automated traffic part I: Theoretical analysis with generalized time geography,” *Transportation Research Part B: Methodological*, vol. 95, pp. 394–420, 2017.
  - [25] K. Dresner and P. Stone, “A multiagent approach to autonomous intersection management,” *Journal of Artificial Intelligence Research*, vol. 31, pp. 591–656, 2008.
  - [26] M. Martin-Gasulla and L. Eleftheriadou, “Traffic management with autonomous and connected vehicles at single-lane roundabouts,” *Transportation Research Part C: Emerging Technologies*, vol. 125, Article ID 102964, 2021.
  - [27] B. Chalaki, L. E. Beaver, and A. A. Malikopoulos, “Experimental validation of a real-time optimal controller for coordination of cavs in a multi-lane roundabout,” in *Proceedings of the 2020 IEEE Intelligent Vehicles Symposium (IV)*, pp. 775–780, IEEE, Las Vegas, NV, USA, October 2020.
  - [28] R. M. James, B. E. Hammit, and S. D. Boyles, “Methods to obtain representative car-following model parameters from trajectory-level data for use in microsimulation,” *Transportation Research Record: Journal of the Transportation Research Board*, vol. 2673, no. 7, pp. 62–73, 2019.
  - [29] L. Xiao, M. Wang, W. Schakel, and B. van Arem, “Unravelling effects of cooperative adaptive cruise control deactivation on traffic flow characteristics at merging bottlenecks,” *Transportation Research Part C: Emerging Technologies*, vol. 96, pp. 380–397, 2018.
  - [30] S. Tsugawa, S. Jeschke, and S. E. Shladover, “A review of truck platooning projects for energy savings,” *IEEE Transactions on Intelligent Vehicles*, vol. 1, no. 1, pp. 68–77, 2016.
  - [31] Y. Feng, C. Yu, and H. X. Liu, “Spatiotemporal intersection control in a connected and automated vehicle environment,” *Transportation Research Part C: Emerging Technologies*, vol. 89, pp. 364–383, 2018.
  - [32] C. Yu, Y. Feng, H. X. Liu, W. Ma, and X. Yang, “Integrated optimization of traffic signals and vehicle trajectories at isolated urban intersections,” *Transportation Research Part B: Methodological*, vol. 112, pp. 89–112, 2018.
  - [33] Q. Ye, X. Chen, R. Liao, and L. Yu, “Development and evaluation of a vehicle platoon guidance strategy at signalized intersections considering fuel savings,” *Transportation Research Part D: Transport and Environment*, vol. 77, pp. 120–131, 2019.
  - [34] S. Bang and S. Ahn, “Platooning strategy for connected and autonomous vehicles: transition from light traffic,” *Transportation Research Record: Journal of the Transportation Research Board*, vol. 2623, no. 1, pp. 73–81, 2017.
  - [35] F. Ma, Y. Yang, J. Wang et al., “Eco-driving-based cooperative adaptive cruise control of connected vehicles platoon at signalized intersections,” *Transportation Research Part D: Transport and Environment*, vol. 92, Article ID 102746, 2021.
  - [36] J. N. Hooker, A. B. Rose, and G. F. Roberts, “Optimal control of automobiles for fuel economy,” *Transportation Science*, vol. 17, no. 2, pp. 146–167, 1983.
  - [37] X. He, H. X. Liu, and X. Liu, “Optimal vehicle speed trajectory on a signalized arterial with consideration of queue,” *Transportation Research Part C: Emerging Technologies*, vol. 61, pp. 106–120, 2015.
  - [38] K. Katsaros, R. Kernchen, M. Dianati, and D. Rieck, “July. Performance study of a Green Light Optimized Speed Advisory (GLOSA) application using an integrated cooperative ITS simulation platform,” in *Proceedings of the 2011 7th International Wireless Communications and Mobile Computing Conference*, pp. 918–923, IEEE, Istanbul, Turkey, July 2011.
  - [39] R. Stahlmann, M. Möller, A. Brauer, R. German, and D. Eckhoff, “Exploring GLOSA systems in the field: technical evaluation and results,” *Computer Communications*, vol. 120, pp. 112–124, 2018.
  - [40] M. Treiber, A. Hennecke, and D. Helbing, “Microscopic simulation of congested traffic,” *Traffic and Granular Flow '99*, Springer, Salmon, NY, USA, pp. 365–376, 2000.
  - [41] W. Do, O. M. Rouhani, and L. Miranda-Moreno, “Simulation-based connected and automated vehicle models on highway sections: a literature review,” *Journal of Advanced Transportation*, vol. 2019, Article ID 9343705, 14 pages, 2019.
  - [42] Z.-w. Yi, W.-q. Lu, L.-h. Xu, X. Qu, and B. Ran, “Intelligent back-looking distance driver model and stability analysis for connected and automated vehicles,” *Journal of Central South University*, vol. 27, no. 11, pp. 3499–3512, 2020.
  - [43] T. Ma and B. Abdulhai, “Genetic algorithm-based optimization approach and generic tool for calibrating traffic

- microscopic simulation parameters,” *Transportation Research Record: Journal of the Transportation Research Board*, vol. 1800, no. 1, pp. 6–15, 2002.
- [44] J. Erdmann, “SUMO’s lane-changing model,” in *Modeling Mobility with Open Data*, pp. 105–123, Springer, Salmon, NY, USA, 2015.
- [45] D. Krajzewicz, M. Behrisch, P. Wagner, R. Luz, and M. Krumnow, “Second generation of pollutant emission models for SUMO,” *Modeling Mobility with Open Data*, pp. 203–221, Springer, Berlin, Germany, 2015.
- [46] A. Alam, B. Besselink, V. Turri, J. Mårtensson, and K. H. Johansson, “Heavy-duty vehicle platooning for sustainable freight transportation: a cooperative method to enhance safety and efficiency,” *IEEE Control Systems Magazine*, vol. 35, no. 6, pp. 34–56, 2015.
- [47] M. Yu and W. D. Fan, “Optimal variable speed limit control in connected autonomous vehicle environment for relieving freeway congestion,” *Journal of Transportation Engineering, Part A: Systems*, vol. 145, no. 4, Article ID 04019007, 2019.